ELSEVIER

Intermetallics 8 (2000) 1119–1129

Intermetallics

www.elsevier.com/locate/intermet

Physical metallurgy and mechanical properties of transition-metal Laves phase alloys

C.T. Liu *, J.H. Zhu [1], M.P. Brady, C.G. McKamey, L.M. Pike [2]

Metals and Ceramics Division, Oak Ridge National Laboratory, Oak Ridge, TN 37831-6115, USA

Received 1 March 2000; accepted 15 August 2000

Abstract

This paper provides a comprehensive review of the recent research on the phase stability, point defects, and fracture toughness of AB_2 Laves phases, and on the alloy design of dual-phase alloys based on a soft Cr solid solution reinforced with hard XCr_2 second phases (where X = Nb, Ta and Zr). Anti-site defects were detected on both sides of the stoichiometric composition of $NbCr_2$, $NbCo_2$, and $NbFe_2$, while they were observed only on the Co-rich side of $ZrCo_2$. Only thermal vacancies were detected in the Laves phase alloys quenched from high temperatures. The room-temperature fracture toughness cannot be effectively improved by increasing thermal vacancy or reducing stacking fault energy through control of phase stability. Microstructures, mechanical properties, and oxidation resistance of dual-phase alloys based on Cr–$NbCr_2$, Cr–$TaCr_2$, and Cr–$ZrCr_2$ were studied as functions of heat treatment and test temperature at temperatures to 1200°C. Among the three alloy systems, Cr–$TaCr_2$ alloys possess the best combination of mechanical and metallurgical properties for structural use at elevated temperatures. © 2000 Published by Elsevier Science Ltd.

Keywords: A. Laves phases; B. Mechanical properties at high temperatures; B. Mechanical properties at ambient temperature; D. Defects: point defects

1. Introduction

Laves phases with AB_2 compositions are a common type of topologically close-packed (TCP) structures [1–4]. There are over 360 binary Laves phases reported in the literature. Furthermore, Laves phases are capable of dissolving considerable amounts of ternary alloying additions. A total of over 900 combined binary and ternary Laves phases have been documented. Although Laves structures are the most abundant among intermetallic compounds, they are the least investigated. So far, most previous studies on intermetallic alloys have concentrated on simple ordered structures derived from face-centered cubic (f.c.c.), body-centered cubic (b.c.c.), or hexagonal-close packed (h.c.p.) structures. Thus, there is a great need for the study of Laves phase alloys.

There are three common polytypes of Laves phases most frequently observed: cubic C15, hexagonal C14 and dihexagonal C36 [1–4]. These polytypes are related to each other as the basic unit layer of these phases is the same, while the stacking sequence of the unit layer is different in each structure. One unit layer in each Laves phase is composed of four sub-layers. In the C15 structure, the packing sequence of the unit layer is ABCABC, similar to the sequence in conventional cubic f.c.c. metals; in the hexagonal C14, the packing layer is ABABABAB, similar to the sequence in conventional h.c.p. metals. The dihexagonal C36 structure has a packing sequence of ABACABAC.

Laves phases are generally stabilized by the size-factor principles, that is, the atomic size ratio, R_A/R_B, is ideally 1.225, with a range of 1.05–1.68 usually observed [1–4]. The stability of each crystalline structure is also influenced by the electron concentration factor (e/a) [5,6]. In fact, the electron concentration factor becomes clearly important when the atomic size factors are favorable. The classic work by Laves and Witte [5,6] showed that for several quasi-binary alloy systems involving $MgCu_2$ and $MgZn_2$, with increasing valence electron concentration, the three Laves types, $MgCu_2$, $MgNi_2$, and $MgZn_2$, exist in that order.

* Corresponding author.

[1] Present address: Tennessee Technology University, TTU Box 5014, Cookeville, TN 38505-0001, USA.

[2] Present address: Haynes International, Kokomo, IN 46904, USA.

0966-9795/00/$ - see front matter © 2000 Published by Elsevier Science Ltd.
PII: S0966-9795(00)00109-6

Laves phases are an important and attractive type of material both scientifically and technologically. They are being seriously considered for many practical applications. For example, $(Tb,Dy)Fe_2$ has been used as a magnetoelastic transducer because of its great magnetorestriction [7]. Compounds of $(Hf,Zr)V_2$ have demonstrated superconducting properties with a combination of high critical temperature, high current density and good magnetic strength [8,9]. Laves phases, such as $Zr(Cr,Fe)_2$, have been considered for hydrogen storage applications due to favorable hydriding-dehydriding kinetics and high hydrogen-absorbing capabilities [10]. The $Mo(Co,Si)_2$ Laves phase contributes to the wear-resistance of "Tribaloy" materials [11]. More recently, $HfCr_2$-, $NbCr_2$- and $TiCr_2$-based two-phase alloys are being developed for high-temperature structural uses because of their high melting points and good retention of mechanical properties at elevated temperatures [12–20].

Despite their useful properties, the low ductility and brittle fracture characteristics at ambient temperatures are the main limitations for structural applications of this large class of alloys. The high hardness and brittle fracture of Laves phases are due to the complex atomic configuration of each unit layer, interplanar locking and lack of operating slip systems at ambient temperatures. Recently, a synchroshear mechanism [21] has been proposed to facilitate plastic deformation in Laves phases, which raises the hope of toughening the Laves phases, even though so far no experimental support for this mechanism has been furnished. All these facts indicate that more research needs to be undertaken on Laves phases in order to further understand the basic phase stability, defect structure, deformation mechanism and fracture behavior. Moreover, alloy design efforts should be devoted to overcoming the brittleness in these phases.

This paper summarizes our recent studies of single-phase and dual-phase alloys containing transition-metal elements. The phase stability and defect structures in Laves phases $NbCr_2$, $NbFe_2$, $NbCo_2$ and $ZrCo_2$ have been studied for the purposes of (1) promotion of synchroshear deformation by increasing vacancy concentration and (2) promotion of mechanical twinning by controlling phase stability and reducing stacking fault energy. At present only limited progress has been achieved in improving the fracture toughness of these Laves phase alloys. In view of this problem, dual-phase alloys based on a soft Cr-rich solid solution reinforced with hard $NbCr_2$, $ZrCr_2$, or $TaCr_2$ second phases have been selected for alloy development [17,22–26]. Among the three Cr–XCr_2 (X = Nb, Zr, and Ta) systems, Cr–$TaCr_2$ alloys are more resistant to air oxidation and thermally-induced cracking. As a result, our current alloy development effort has been focusing on the Cr–$TaCr_2$ alloy system, and significant advances have been made in enhancing the high-temperature strength, creep resistance and fracture toughness of the dual-phase alloys through compositional adjustment, microstructural control and alloy additions.

2. Point defect and fracture toughness of binary Laves phases

Laves phases are generally considered to be line compounds with a strict AB_2 composition. However, solubility ranges exist for about 25% of the known binary Laves phases [27]. For non-stoichiometric compositions, constitutional defects are incorporated into intermetallic compounds. However, for the Laves phases, little is known about the possible defect structures that may be associated with the deviations from stoichiometry. The excess atoms in off-stoichiometric compounds can stay on their own sublattice (leading to the formation of constitutional vacancies on the other sublattice), insert into interstitial sites, or occupy sites on the other sublattice (anti-site substitution). Since Laves phases have TCP structures and space-filling is relatively high, there are no interstitial sites with a size comparable to that of the component atoms. Therefore, the insertion of the excess atoms into interstitial sites can be excluded, and the possible defect mechanisms in binary Laves phases reduce to either constitutional vacancy or anti-site substitution.

The Laves phases are known to be size compounds, i.e. the atomic size ratio, R_A/R_B is ideally 1.225, with a range of 1.05–1.67 typically observed. Since the A atom is much larger than the B atom, the excess A atoms in A-rich compositions would tend to stay on their own sublattice sites, thus creating vacancies on the B atom sublattice. On the other hand, the excess B atoms on B-rich compositions would be able to occupy the A atom sublattice sites, leading to the formation of anti-site defects. Based on these geometric arguments, it has been postulated that the A-rich side is accommodated by vacancies, while the B-rich compositions result from the anti-site substitution [27]. However, no systematic experimental verification has been undertaken so far.

The types of constitutional defects may affect physical, mechanical and functional properties of Laves phases. Vacancies have been proposed to assist the movement of synchro-Shockley dislocations [21], thus possibly facilitating the synchroshear deformation mechanism and increasing the toughness of Laves phases [28]. Off-stoichiometry was also found to affect the hydride stability of $ZrMn_2$ [29] and the hydrogen storage capability of $TiMn_2$ alloys [30]. The defect structures of the cubic C15 $NbCr_2$, $NbCo_2$ and $ZrCo_2$ and hexagonal C14 $NbFe_2$ Laves phases were studied to clarify the point defect mechanisms on both sides of stoichiometry in these binary systems. This was done by measuring the lattice parameters, bulk densities, and therefore, vacancy concentrations of these alloys of various compositions

[31,32]. The hardness of the above alloys with various point defect concentrations was determined in an attempt to explore the solid solution hardening behavior in the Laves phases. The fracture toughness was also measured to investigate whether the point defects affect the toughness of the alloys, and, in particular, to see if vacancies facilitate synchroshear deformation in the vacancy-containing alloys.

Figs. 1 and 2 show the vacancy concentration as a function of the Nb content for $NbCr_2$ and $NbFe_2$ alloys, respectively, after quenching from different temperatures [31]. It is clear that after quenching the $NbCr_2$ alloys from 1000°C, the vacancy concentration is essentially zero, while the vacancy concentration significantly increases after quenching from higher temperatures, i.e. 1400°C. For the $NbFe_2$ alloy, the vancancy concentration is very low even after quenching from 1300°C. Fig. 3 summarizes all the measured vacancy concentrations for all single-phase alloys after quenching from 1000°C, which are essentially zero. The calculated vacancy concentrations from both the constitutional vacancy model and anti-site substitution model are also plotted in Fig. 3 [31]. The experimental results indicate that there are no constitutional vacancies in these Laves phases on either side of stoichiometry. This is consistent with the anti-site substitution model and contrary to the constitutional vacancy model, which demands much higher vacancy concentrations for off-stoichiometric compositions. Note that the constitutional vacancy model is based on the assumption that all the excess atoms exclusively stay on their own sublattice, thus constitutional vacancies are created on the sublattice of the other element. The anti-site substitutional model assumes that the excess atoms occupy the sublattice sites of the other species. As a result, anti-site defects are created, and no constitutional vacancies are needed for the balance of the lattice sites. Thus, the constitutional defects on the Cr-, Co-, or Fe-rich, as well as the Nb-rich sides of stoichiometry, are of anti-site type for the $NbCr_2$, $NbCo_2$ and $NbFe_2$ Laves phases.

Modder and Bakker pointed out that it is very possible that a vacancy type defect, termed quadruple defect, occurs in C15 compounds [33]. Such a quadruple defect consists of one anti-site B atom on the α sublattice and three vacancies on the β sublattice. Ball milling was found to introduce quadruple defects in $GdAl_2$, $GdPt_2$, $GdIr_2$ and $GdRh_2$, while anti-site defects were created in $GdMg_2$ after ball-milling [34]. Since ballistic actions such as ball milling usually lead to the formation of the same type of atomic defects as heating, thermal defects such as quadruple defects or anti-site defects may be created upon quenching the Laves compounds from elevated temperatures. Thermal vacancies are expected

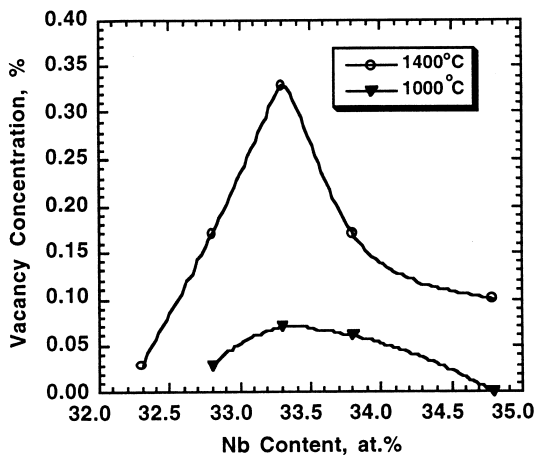

Fig. 1. Vacancy concentration vs Nb content for $NbCr_2$ Laves phase quenched from 1000 and 1400°C [31].

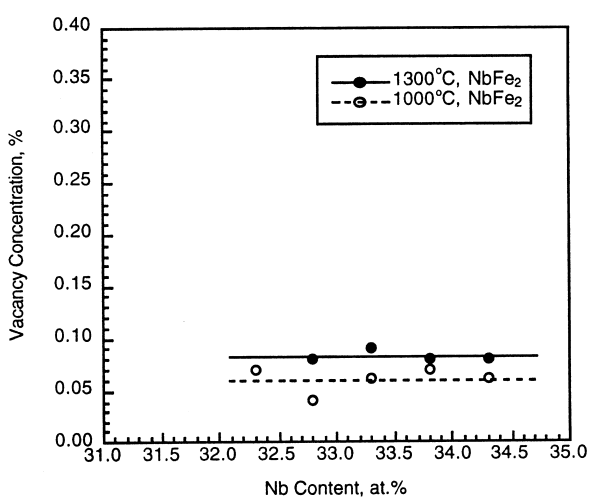

Fig. 2. Vacancy concentration vs Nb content for $NbFe_2$, Laves phase quenched from 1300 and 1000°C [31].

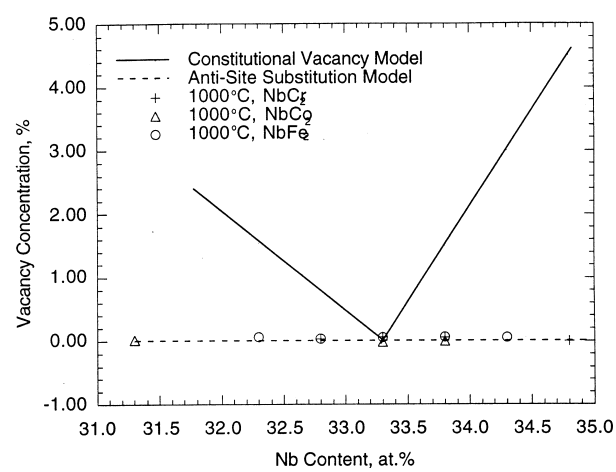

Fig. 3. Measured vacancy concentration vs Nb content in the binary $NbCr_2$, $NbCo_2$, and $NbFe_2$, Laves phases after quenching from 1000°C. Also shown are the calculated data for the constitutional vacancy model and the anti-site substitution model [31].

if quadruple defects are created, as each quadruple defect contains three vacancies.

It is interesting to note that appreciable vacancies were detected in the $NbCr_2$ alloy after quenching from 1400°C (Fig. 1). Since these vacancies were essentially annealed out at 1000°C (Fig. 1), and since the constitutional defects in this compound have been established to be of the anti-site type, it is concluded that these defects are *thermal* vacancies, indicating that quadruple defects may be formed in this compound by heating. Furthermore, the measured vacancy concentration exhibits a maximum at the stoichiometric composition and decreases on both sides of stoichiometry for the $NbCr_2$ alloys when quenched from 1400°C (Fig. 1). A maximum in thermal vacancy concentration, and thus thermal disorder, at the stoichiometric composition can be rationalized by considering the fact that the increase in entropy associated with the introduction of vacancies is the greatest at the stoichiometric composition where the degree of order is necessarily the highest.

For the C14 $NbFe_2$ compounds, no thermal vacancies were detected after quenching from 1300°C (Fig. 2), indicating that anti-site defects, instead of quadruple defects, may be the form of atomic disorder in this compound upon heating. According to the model developed by Modder et al. [34], the type of atomic disorder is related to the relative magnitudes of formation enthalpies of anti-site and quadruple-defect disorder for the Laves phases. Therefore, the differences in thermal defects in $NbCr_2$ and $NbFe_2$ imply that the formation enthalpies of anti-site disorder are larger in magnitude than that of the quadruple defect disorder for $NbCr_2$, while the opposite is true for $NbFe_2$.

A point defect in a crystalline lattice is well known to cause hardening. This phenomenon is referred to as solid solution hardening. Solid solution hardening has been extensively studied in B2 compounds [35]. Generally, it is found that in B2 compounds with anti-site defects, hardness exhibits a minimum at the stoichiometric composition, and deviation from stoichiometry causes hardening of the compounds, due to the presence of constitutional anti-site defects. For triple-defect B2 compounds, the shape of the hardness versus composition curves was found to be not so simple and depended on the degree of thermal disorder. Also, vacancies were found to be a more potent hardener than the anti-site defects.

In the $NbCr_2$ and $NbFe_2$ Laves phases studied, the hardness was also found to have a characteristic V-shape with a minimum occurring at the stoichiometric compositions (Figs. 4 and 5) [31]. Obviously, similar to anti-site B2 compounds, such off-stoichiometric hardening can be attributed to the presence of constitutional anti-site defects, which is the defect mechanism on both sides of stoichiometry in these Laves phases. The anti-site hardening mechanism in Laves phases, however, is not clear so far, and it may be different from that in B2 compounds. In B2 compounds, the anti-site hardening is often correlated to an interaction between the stress field of a moving dislocation and that of the anti-site

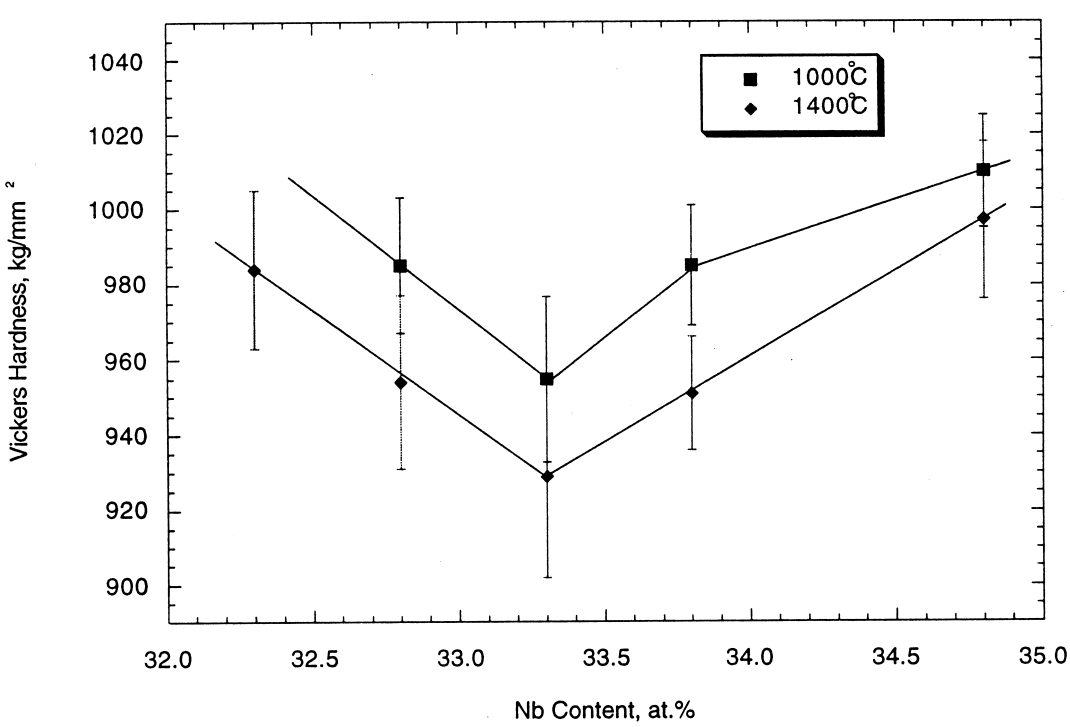

Fig. 4. Vickers hardness vs Nb content for $NbCr_2$ alloys after quenching from 1400 and 1000°C [31].

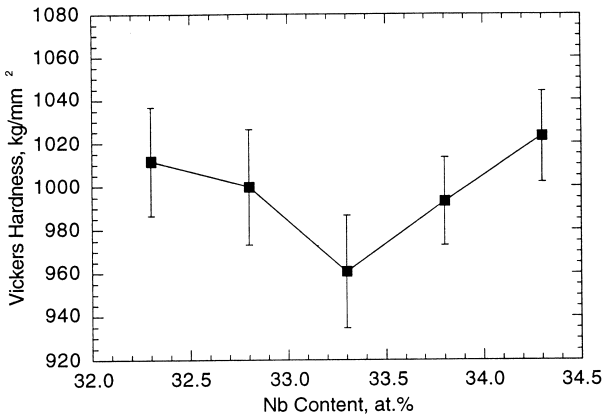

Fig. 5. Vickers hardness vs Nb content for $NbFe_2$ alloys after quenching from 1000°C [31].

defect; however, it is very difficult for ordinary dislocations to move in Laves phases at ambient temperatures.

The hardness values of all $NbCr_2$ alloys after quenching from 1400°C appear to be lower than those after quenching from 1000°C (Fig. 4). Since thermal vacancies are incorporated into the compound after quenching from 1400°C (see Fig. 1), the above results may suggest that vacancies cause softening, instead of hardening of the $NbCr_2$ Laves phases. Such vacancy-induced softening has not been observed previously in other systems. Furthermore, this is in direct contrast to the effect of vacancies on the hardness in B2 compounds, where vacancies are a potent hardener. The vacancy hardening in metals and B2 compounds is often correlated to an interaction between the stress field of a moving dislocation and that of the vacancy. The effect of vacancies in Laves phases may be different from their effects in metals and B2 compounds. This is again likely to be due to the fact that Laves phases have a topologically close-packed structure and it is very difficult for ordinary dislocations to move. The presence of vacancies in Laves phases would make the structure less closely packed and could possibly assist the synchroshear deformation of the alloy [21,36], thus possibly leading to the softening of the alloys.

The fracture toughness values as a function of the Nb content in $NbCr_2$ Laves phases after quenching from 1400 and 1000°C as well as $NbCo_2$ and $NbFe_2$ Laves phases after quenching from 1000°C are plotted in Fig. 6. Basically, the fracture toughness of the $NbCr_2$ and $NbCo_2$ alloys is close to 1 MPa $m^{1/2}$. No effect of stoichiometry on the fracture toughness can be discerned. Even though the anti-site defects harden the Laves phases (Figs. 4 and 5), they are not detrimental to the fracture toughness of the alloys. Furthermore, it is noted that the fracture toughness of the $NbCr_2$ alloys after quenching from 1400°C is similar to that of the alloys after quenching from 1000°C, i.e. the presence of thermal vacancies (<0.4%) does not lead to an improved toughness of the Laves phases, even though the vacancies slightly soften the Laves phases (see Fig. 4). Similar results were observed for $ZrCo_2$ alloys quenched from different temperatures [32]. The fracture toughness of the C14 $NbFe_2$ alloys is lower than that of C15 $NbCr_2$ and $NbCo_2$. This trend can be explained by the fact that the C15 structure is cubic, and is possibly more deformable than the hexagonal C14 structure.

It has been suggested that vacancies in Laves phases may assist the synchroshear mechanism, thus leading to improvement in the deformability and toughness of the Laves alloys [21,36]. Chen et al. [28] attributed the toughness improvement in the off-stoichiometric $TiCr_2$ alloys to the presence of vacancies in the alloys. The quenched-in thermal vacancies do not affect the crack propagation and fracture toughness behavior of the $NbCr_2$ alloys (Fig. 6). This is possibly due to the fact that the level of vacancies is too low in the alloys to enhance toughness significantly. It is also possible that the high residual thermal stress after quenching from 1400°C may also embrittle the $NbCr_2$ Laves phases, and thus could mask the effect of vacancy-assisted synchroshear deformation and its associated toughening.

The atomic size ratio, R_A/R_B, of the AB_2 Laves phases studied can be calculated to be 1.145, 1.173, and 1.152 for $NbCr_2$, $NbCo_2$, and $NbFe_2$, respectively. Here, R_A and R_B are the atomic radii of the A and B atoms with a coordination number of 12. Obviously, all the Laves phases studied have R_A/R_B ratios smaller than the ideal ratio of 1.225 for Laves-phase formation. It will be interesting to know the defect mechanism for Laves phases with R_A/R_B greater than 1.225. It may be easier to obtain constitutional vacancies for Laves phases with $R_A/R_B > 1.225$, due to geometric considerations, i.e. it is more difficult for A atoms to stay on the sublattice sites of B atoms as the atomic size ratio increases. On the other hand, it has been found that for the B2 phases, the

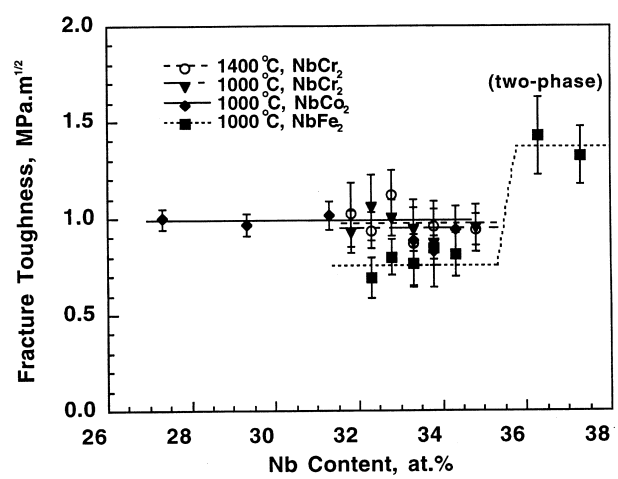

Fig. 6. Fracture toughness vs Nb content for binary $NbCr_2$, $NbCo_2$ and $NbFe_2$ Laves-phase alloys. Note two of the $NbFe_2$ alloys are not single Laves phase [31].

defect type is closely related to the enthalpies of formation (ΔH) of the compounds. Neumann has demonstrated that B2 compounds with negative ΔH smaller than 75–90 kJ/mol generally exhibit the anti-site defect structure, while compounds with a greater value generally exhibit the triple defect structure and have constitutional vacancies on the large-atom side of stoichiometry [37]. In other words, constitutional vacancies are the preferred defect mechanism in compounds that are more strongly ordered, i.e. with higher absolute ΔH values on the large-atom side. This empirical observation may be extended to the binary Laves phases. The ΔH values for $NbCr_2$, $NbCo_2$, and $NbFe_2$ are −21, −51, and −63 kJ/mol, respectively [38]. These values are in the same range as those of B2 compounds with anti-site defects. It is not surprising that only anti-site defects are observed in these Laves phases. Based on such geometric and thermodynamic considerations, future work should be concentrated on Laves phases with high R_A/R_B ratios and/or large negative enthalpies of formation. One such Laves phase is $ZrCo_2$, which has a large difference in atomic size between component atoms ($R_A/R_B = 1.28$) and an enthalpy-of-formation value of −123 kJ/mol [32]. Recent results indicate that a second phase, instead of constitutional vacancies, is formed in $ZrCo_2$ alloys with Zr > 33.3%. Interestingly, thermal vacancy concentrations in $ZrCo_2$ alloys of near stoichiometric composition are as high as 1%, see Fig. 7 [32]. These vacancies do not affect fracture toughness.

3. Phase stability and fracture toughness of transition-metal Laves phases

As mentioned above, the different Laves phase polytypes are a result of different stacking sequences. The stacking fault energy is expected to be lower at phase boundaries (e.g. C14/C15 boundary), where mechanical twinning becomes more easily triggered.

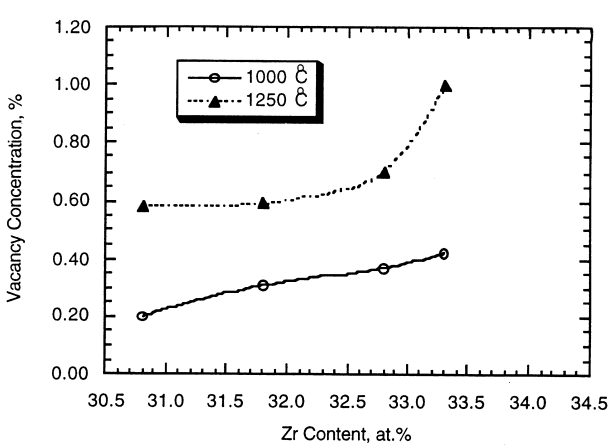

Fig. 7. Vacancy concentration vs Zr content for $ZrCo_2$ Laves phase quenched from 1000 and 1250°C [32].

The stability ranges of the Laves phases in both binary and ternary systems were obtained from phase diagram information, and the e/a effect on the phase stability (C14/C15) in $NbCr_2$-based transition-metal Laves phases is shown in Fig. 8 [39,40]. In the $NbCr_2$-based Laves phases, the e/a ratio for the C15/C14 phase boundaries is quite precise; the critical e/a values, corresponding to the C15/C14/C15 phase transitions from the phase diagram information (as indicated in Fig. 8), are as follows: at e/a values lower than 5.76, the C15 structure is stabilized for both binary and ternary Laves alloys; by increasing e/a to 5.88, the C14 structure is stabilized; over the e/a range of 5.88–7.53, the C14 structure is more stable than the C15 structure; the C15 structure is stabilized again over the C14 structure when the e/a ratio is increased further to 7.65 for the Nb–Cr–Co system. In the ternary Nb–Cr–Fe system, such a C14→C15 transition was not observed, since the highest e/a ratio was 6.69 in this system (Fig. 8). No $NbNi_2$ (with e/a = 8.34) or $NbCu_2$ (with e/a = 9) Laves phases exist in binary Nb–Ni and Nb–Cu systems (the e/a values for imaginary "$NbNi_2$" and "$NbCu_2$" were shown in Fig. 8), consistent with the observation by Bardos et al. [41] that at e/a > 8, a disordered structure is stabilized over the Laves phase in transition-metal systems.

The phase stability in pseudo-binary $Nb(Cr,Fe)_2$ and $Nb(Cr,Co)_2$ systems was also studied experimentally and good agreement between the experimental results and surveyed data based on phase diagram information was observed, as shown in Fig. 8. It is clear that the electron concentration rule is obeyed in these two pseudo-binary systems: the phase transitions between C15 and C14 are determined by the average electron concentration in these alloys. The experimental critical e/a ratios for the C15/C14/C15 transitions are very close to those from phase diagrams. These results were the first experimental determination of the critical e/a values for the different Laves phases in the pseudo-binary $Nb(Cr,X)_2$ systems. Such good agreement may be associated with the fact that all the components in the two

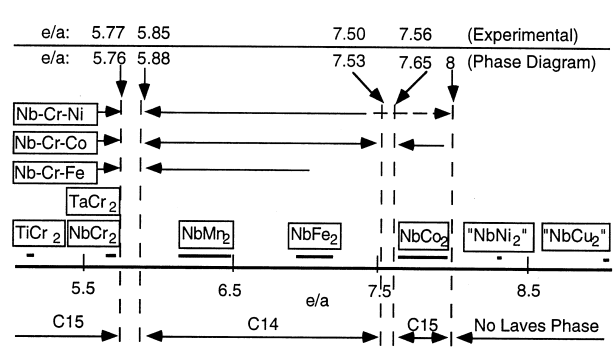

Fig. 8. Effect of average electron concentration (e/a) on phase stability in $NbCr_2$-based systems, with the critical e/a values for phase transitions both from phase diagram information and experimental data [40].

pseudo-binary systems are transition metals. Furthermore, it is determined that the region between C14 and C15 is a two-phase mixture of C14 and C15, with no intermediate structures such as C36 observed.

The effect of Fe and Co contents on the fracture toughness of $Nb(Cr,X)_2$ Laves phase is shown in Figs. 9 and 10, respectively [40]. Basically, the fracture toughness of the monolithic Laves phase is very low, around 1 MPa$\sqrt{m}$, which is a consequence of the topologically close packing manner of the structure and the subsequent difficulty in activating dislocation sources in the Laves phase. The cubic C15 phase has relatively higher fracture toughness than that of C14 structure for the ternary systems, regardless of the Fe or Co addition. This can be explained by the fact that the C15 structure is cubic, and is thus more deformable than the hexagonal C14 structure. The toughness value near the phase boundary could be higher, in view of the fact that the associated structure is metastable with a lower stacking fault energy, thus possibly making stress-assisted phase transformation and/or mechanical twinning easily triggered during deformation. However, such a trend was not observed in the present study. None of the alloys within the two-phase regions or near the phase boundaries exhibits any sign of increase in toughness. The toughness of the two-phase (C14 + C15) alloys is similar to that of the C15 phase. The toughness enhancement through stress-assisted phase transformation or mechanical twinning is not significant enough to be noted in the indentation test.

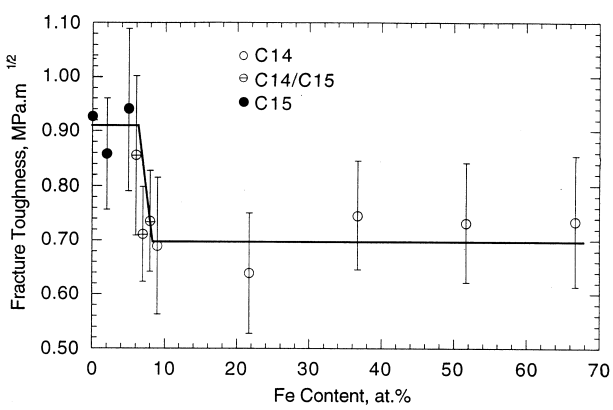

Fig. 9. Fracture toughness values of $Nb(Cr,Fe)_2$ as a function of the Fe content [40].

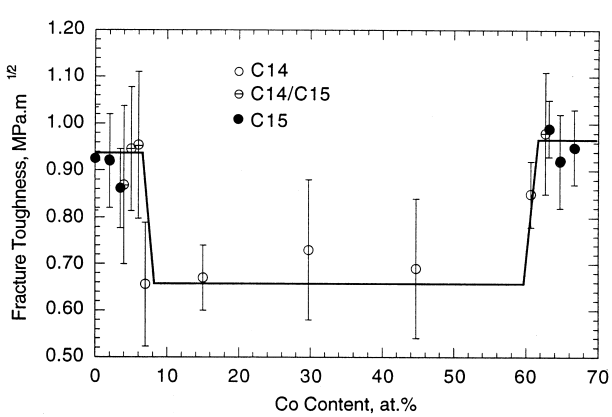

Fig. 10. Fracture toughness values of $Nb(Cr,Co)_2$ as a function of the Co content [40].

4. Alloy design of dual-phase Cr-XCr_2 alloys

As indicated in the forgoing two sections, single-phase Laves phase alloys with cubic C15 and hexagonal C14 are hard and brittle, and their fracture toughness at ambient temperatures can not be effectively improved using physical metallurgy principles, including control of point defect and phase stability. In view of this, dual-phase alloys based on a soft Cr-rich solid solution reinforced with hard Laves phase second phases have been selected for alloy development [17,22–26] for potential structural use at elevated temperatures. This section summarizes the progress made so far in the development of dual-phase Cr–XCr_2 alloys, where X = Nb, Ta, or Zr.

Three eutectic alloy systems, Cr–$NbCr_2$, Cr–$TaCr_2$, and Cr–$ZrCr_2$, were initially selected for alloy development study. The selection is based on consideration of the different eutectic phase relationships in these alloy systems [16,25,26,42], as indicated in Table 1. Fig. 11 shows the Cr–$TaCr_2$ phase diagram which is typical for the three eutectic systems. Among these systems, the Cr–Nb system has the highest maximum solute solubility (5.6% Nb) in the Cr solid solution and the highest solute concentration in the eutectic composition (18.5% Nb), whereas the Cr–Zr system has the least maximum solute solubility (< 0.6% Zr) in Cr and the Cr–Ta system has the lowest solute concentration in the eutectic composition (9.8% Ta). These alloy parameters are expected to strongly affect the hardening behavior of both the Cr solid solution phase and the eutectic structure and thus the degree of brittleness of these phases.

Alloy ingots containing up to 20 at. % X element were prepared by arc melting and drop casting, using pure metal elements. In order to control precipitation reactions, alloy ingots were sectioned and heat treated between 1000 and 1400°C. The first interesting observation was that alloy ingots were quite often cracked for Cr–$NbCr_2$ alloys but not for Cr–$TaCr_2$ and Cr–$ZrCr_2$

Table 1
Alloy parameters existing in the three eutectic systems Cr–Nb, Cr–Ta and Cr–Zr

Alloy parameter	Cr–Nb	Cr–Ta	Cr–Zr
Eutectic temperature (C°)	1703	1760	1592
Max. solute solubility in Cr (at%)	5.6 Nb	~4.0 Ta	< 0.6 Zr
Eutectic composition (at%)	18.5 Nb	9.8 Ta	~18.0 Zr

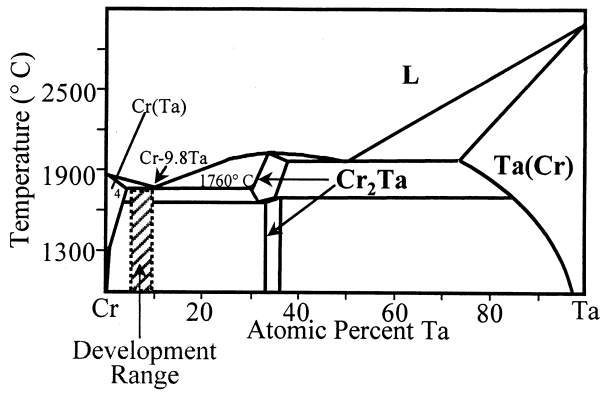

Fig. 11. Schematic binary Cr–Ta phase diagram.

alloys during drop casting and cooling from heat treatment at high temperatures. This cracking behavior cannot be simply related to the difference in coefficients in thermal expansion (CTE) because both experimental measurements and first principle calculations [43–45] indicate no major difference in CTE among the Laves phases $NbCr_2$, $TaCr_2$ and $ZrCr_2$. The cracking behavior, on the other hand, can be better rationalized by considering alloy parameters in the three eutectic systems. As indicated in Table 1, the maximum solute solubility in Cr and the solute concentration in the eutectic structures (which increases the proportion of the hard Laves phases in the eutectic microstructure) are the highest in the Cr–$NbCr_2$ system, resulting in significant hardening and embrittlement of the primary Cr solid solution phase and the eutectic composition. In this case, tremendous hardening is induced from fast cooling from the maximum-solubility temperature to lower temperatures where the primary Cr solid solution is in supersaturated states. As a result, thermal induced stresses generated by CTE mismatch will high enough to crack these phases during drop casting or cooling from high temperatures [46,47], quite often resulting in catastrophic ingot failure. This study clearly indicates the importance of phase relationship that may provide key information governing the mechanical and metallurgical behaviors of individual alloy phases.

In comparison with the dual-phase Cr–$TaCr_2$ alloys, Cr–$ZrCr_2$ alloys suffer from two major problems. One is the poor oxidation resistance of Cr–$ZrCr_2$ alloys, due, in part, to extensive internal oxidation of Zr-rich phases, and the other is the relative low melting point of these alloys (see Table 1). Thus, our alloy development has been concentrated on the Cr–$TaCr_2$ alloy system, and significant progress has been made in improving the mechanical and metallurgical properties of these alloys [26]. The Cr–$TaCr_2$ alloys with enhanced properties have the general compositions (at%) below:

$$\mathrm{Cr}-(6-10)\mathrm{Ta}-(3-6)\mathrm{Mo}-(0.2-1.0)\mathrm{Ti}-(0.5-3.0)\mathrm{Si}-(0.05-0.20)\mathrm{La/Ce}.$$

In these alloys, Mo is added mainly for solid solution hardening the Cr-rich phase, Ti for scavenging interstitials, and Si for both improving oxidation resistance and fracture toughness. Small amounts of reactive elements such as La and Ce are also added for decreased scaling and enhancing the adhesion of oxide scales.

No micro- and macro-cracks were observed in the Cr–$TaCr_2$ alloy ingots prepared by arc-melting and drop casting. In order to control microstructures, some dual-phase alloys were canned in Mo billets and fabricated by hot extrusion at 1480°C. The alloy CN-151 (Cr-9.75Ta-5Mo-0.5Ti-0.01Ce, at. %) with its composition similar to the eutectic composition shows a full lamellar structure in the as-cast condition and a $TaCr_2$-dispersed microstructure in the hot extruded condition (Fig. 12). The mechanical properties with different microstructures were determined in tension as a function of test tem-

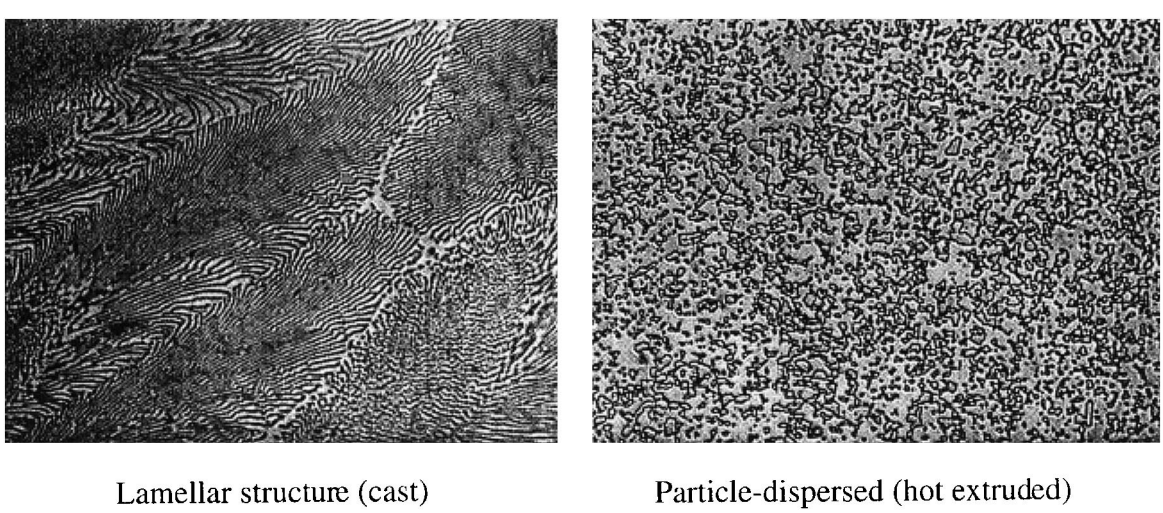

Fig. 12. Comparison of lamellar structure in the cast condition and particle-dispersed microstructure in the hot extruded condition for alloy CN-151.

perature. All tensile specimens were given a final heat treatment of 1 d/1200°C + 1 d/1000°C for stress relief. Note that the heat treatment does not significantly affect the lamellar structure observed in cast alloys.

Table 2 compares the tensile properties of CN-144 alloy with the lamellar and $TaCr_2$-dispersed microstructures. With the dispersed microstructure, the alloy showed a fracture strength of more than 100 ksi (700 MPa), even though no appreciable plastic deformation was measured at room temperature. Plastic deformation was detected at 800°C, and the strain went up to as high as 40% at 1200°C. The alloy is very strong at elevated temperatures, with the yield strength of 37 ksi and the ultimate tensile strength of 46 ksi at 1200°C. Note that the strengths of most Ni-base superalloys vanish at 1200°C. In comparison with the particle-dispersed microstructure, the alloy with the lamellar structure showed the ductile-to-brittle temperature around 1000°C, instead of 800°C. The lamellar structure is extremely strong at 1200°C, with its strengths close to double that for the particle-dispersed microstructure.

The fracture toughness of Cr–$TaCr_2$ alloys with lamellar structures was determined at room temperature, using subsized notched Chevron specimens [48] in accordance with reference 49. The results are summarized in Table 3. The alloy CN-144 with a hypoeutectic composition showed a low fracture toughness of 8.3 MPa $m^{1/2}$. A significant increase in fracture toughness is achieved by increasing the Ta concentration from hypo- to hypereutectic compositions. Alloying with 1.0% Si further increases toughness from 11.5 to 14.3 MPa $m^{-1/2}$. Examination of fracture surfaces reveals that the interfaces between the Cr solid solution and lamellar $TaCr_2$ phases are strong, and no secondary cracks are observed along these interfaces. It is worth noting that hot extrusion and change in microstructures from lamellar to dispersed particles gives no significant increase in fracture toughness.

Table 2
Comparison of tensile properties[a] of CN-144 with lamellar and particle-dispersed microstructures

Test temperature (C°)	Strength (ksi) Yield	Fracture	Elongation (%)
Particle-dispersed microstructure (hot extruded)			
RT	–	104	0.3
800	130	133	1.0
1000	92	103	1.7
1200	37	46	39.0
Lamellar structure (cast)			
RT	–	76	0.2
800	–	–	–
1000	–	80	0.2
1200	68	85	5.3

[a] Tested at a strain rate of 3.3×10^{-3}/s in air.

The creep properties of a Cr–$TaCr_2$ alloy, CN-144 (Cr-8Ta-5Mo-0.5Ti-0.01Ce. at%), were determined in tension at a stress of 20 ksi (138 MPa) at 1000°C in air [26]. Fig. 13 compares the creep curve of CN-144 with the lamellar and dispersed microstructures. The $TaCr_2$ dispersed microstructure exhibited ductile rupture with a rupture life of 695 h at 1000°C. In comparison, the specimen with the lamellar structure is much stronger in creep, with a steady state creep rate lower than that of the particle-dispersed microstructure by an order of magnitude. The test of the lamellar specimen had to be stopped after 1438 h because of grip rod failure. The creep resistance of this alloy in the polycrystalline form with a lamellar structure is stronger than Mar M-200 and DS Rene'80 and is comparable to CMSX-11B in the single crystal form.

The oxidation properties of Cr–XCr_2 alloys were characterized by exposing alloy coupons to air at 900–1100°C. The oxidation studies by Brady et al. [26,50,51] demonstrates that the oxidation resistance of Cr–$TaCr_2$ alloys is much superior to Cr–$NbCr_2$ or Cr–$ZrCr_2$ alloys. Fig. 14 compares the cyclic oxidation behavior of Cr-8Ta alloys with commercial Cr-base alloys tested at

Table 3
Fracture toughness of Cr–Ta alloys at room temperature

Alloy number	Composition[a] (at%)	Fracture toughness (MPa $m^{1/2}$)
CN-144	8.0 Ta–0.01 Ce	8.3
CN-161	9.8 Ta–0.1 La	11.5
CN-145	10.0 Ta–0.01 Ce	12.8
CN-162	9.8 Ta–0.1 La–0.5 Si	11.4
CN-163	9.8 Ta–0.1 La–1.0 Si	14.3

[a] Base composition: Cr-5 Mo-0.5 Ti, at%.

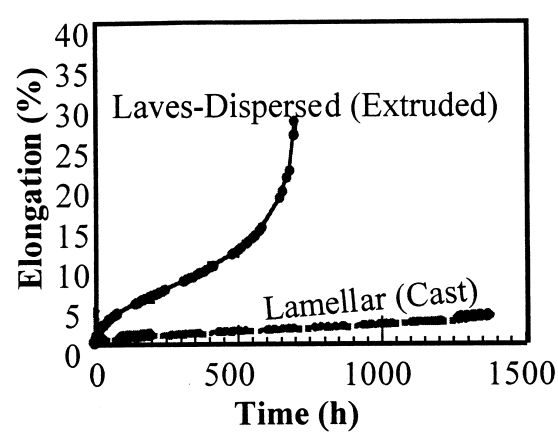

Fig. 13. Comparison of creep properties of CN-144 (Cr-8Ta-5Mo-0.5Ti-0.OlCe, at%) with Laves phase dispersed or lamel lar microstructures tested at 1000°C and 20 ksi in air. Note that the lamellar microstructuie test was stopped due to failure of the grip rods and plate.

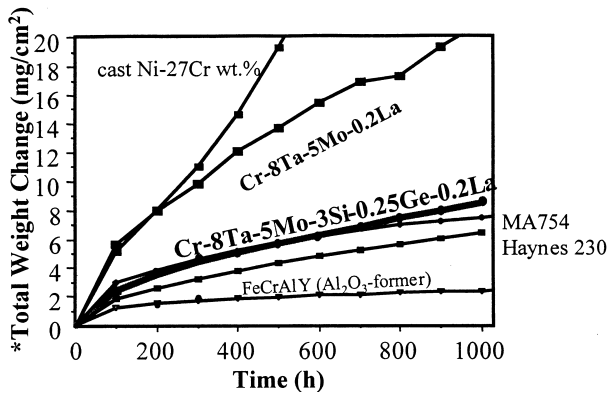

Fig. 14. Comparison of cyclic oxidation of Cr-8Ta alloys with cast Ni-27Cr alloy (wt%) and commercial alloys MA754 and Haynes 230 air oxidized at 1100°C.

1100°C in air [26]. The oxidation rate of Cr-8Ta-5Mo-0.2La is comparable to that of cast Ni-27Cr (wt%), and alloying with additions of Si and Ge significantly lowers the oxidation rate of the Cr–8Ta alloy. As indicated in Fig. 14, the oxidation resistance of Cr-8Ta-5Mo-3Si-0.25Ge-0.2La is comparable to several commercial Cr_2O_3-forming alloys, such as MA-754 and Haynes 230.

5. Conclusions

This paper provides a comprehensive review of phase stability, point defects, and fracture toughness of binary AB2 Laves phase alloys based on $NbCr_2$, $NbFe_2$, $NbCo_2$, and $ZrCo_2$ with on- and off-stoichiometric compositions, and pseudo-binary alloys based on $Nb(Cr,Co)_2$ and $Nb(Cr,Fe)_2$ compositions. The alloy design effort has been concentrated mainly on dual-phase alloys based on a soft Cr-rich solid solution reinforced with hard $TaCr_2$ second phases. Conclusions deduced from these studies are given below:

1. Anti-site defects were observed to form on both sides of the stoichiometry in $NbCr_2$, $NbCo_2$, and $NbFe_2$ with $R_A/R_B < 1.225$. On the other hand, for $ZrCo_2$ with $R_A/R_B > 1.225$, anti-site defects form only on the Co-rich side and second phase particles form on the Zr-rich side.
2. No constitutional vacancies but only thermal vacancies were detected in the Laves phase alloys quenched from high temperatures. The peak vacancy concentration is always located at the stoichiometric composition of each Laves phase alloy.
3. Room-temperature fracture toughness can not be effectively improved either by increasing thermal vacancy concentration at levels below 1% or by reducing stacking fault energy through control of the phase stability in $Nb(Cr,Co)_2$ and $Nb(Cr,Fe)_2$ alloys.
4. Drop casting and heat treatments induce micro- and macro-cracks in dual-phase Cr–$NbCr_2$ alloys but not in Cr–$TaCr_2$, and Cr–$ZrCr_2$ alloys. The cracking behavior can not be simply explained from CTE mismatch; instead, it can be better rationalized from the consideration of eutectic composition and phase relationship.
5. Among the three dual-phase Cr–XCr_2 alloys (where X = Nb, Ta, or Zr), Cr–$TaCr_2$ alloys have the best combination of mechanical and metallurgical properties for structural use at elevated temperatures. These alloys have excellent tensile strength, creep properties, and oxidation resistance at elevated temperatures in air.
6. The alloy design effort has led to the identification of alloy compositions (at%) with enhanced mechanical and metallurgical properties:

$$\mathrm{Cr} - (6-10)\mathrm{Ta} - (3-6)\mathrm{Mo} - (0.2-1.0)\mathrm{Ti} - (0.5-3.0)\mathrm{Si} - (0.05-0.20)\mathrm{La/Ce}.$$

7. The current Cr–$TaCr_2$ alloys showed fracture toughness up to 14.3 M Pa $m^{-1/2}$ at room temperature. Additional development is required to further improve the fracture resistance of these alloys by interfacial design and microalloying.

Acknowledgements

This research was sponsored jointly by the Division of Materials Sciences and Engineering, and the Fossil Energy AR&TD Materials Program, US Department of Energy under contract DE-AC05-00OR22725 with UT-Battelle, LLC. The authors would like to thank L. Heatherly and D. S. Easton for hot extrusion, J. L. Wright for mechanical testing, and C. A. Carmichael for alloy preparation.

References

[1] Laves F. Theory of alloy phases. Metals Park, OH: American Society for Metals, 1956. p. 124
[2] Wernick JH. In: Westbrook JH, editor. Intermetallic compounds. New York: Wiley, 1967. p. 197.
[3] Sinha AK. Progr Mater Sci 1972;15(2):79.
[4] Massalski TB. In: Cahn RW, Hassen P, editors. Physical metallurgy part 1. New York: North-Holland, 1983. p. 190.
[5] Laves F, Witte H. Metallwirschaft 1935;14:645.
[6] Laves F, Witte H. Metallwirschaft 1936;15:840.
[7] Moffett MB, Clark AE, Wun-Fogle M, Lindberg J, Teter JB, McLaughlin EA. J Acoust Soc Am 1991;89:1448.
[8] Inoue K, Tachikawa K. IEEE Trans Magnetics 1979;15:635.
[9] Olzi E, Matacotta FC, Setina P. J Less-Common Met 1988;139:123.
[10] Ivey D, Northwood D. J Less-Common Met 1986;115:23.
[11] Halstead A, Rawlings RD. J. Mater. Sci. 1985;20:1248 & 1693
[12] Anton DL, Shah DM. Mater Res Soc Symp Proc 1990;194:45.

[13] Livingston JD. Phys Status Solidi (a) 1992;131:415.
[14] Chu F, Pope DP. Mater Sci Engng 1993;A170:39.
[15] Kumar KS, Miracle DN. Intermetallics 1994;2:257.
[16] Thoma DJ, Perepezko JH. Mater Sci Engng 1992;A156:97.
[17] Takeyama M, Liu CT. Mater Sci Engng 1991;A132:61.
[18] Chan KS, Davidson DL. JOM 1996;48:62.
[19] Fleischer RL, Zabala RJ. Metall Trans 1990;21A:2149.
[20] Chen KC, Allen SM, Livingston JD. J Mater Res 1997;12:1472.
[21] Hazzledine PM, Kumar KS, Miracle DB, Jackson AG. MRS Symp Proc 1992;288:591.
[22] Liu CT, Tortorelli PF, Horton JA, Carmichael CA. Mater Sci Engng 1996;A214:23.
[23] Kumar KS, Liu CT. Acta Mater 1997;45:3671.
[24] Takasuqi T, Kumar KS, Liu CT, Lee EH. Mater Sci Engng 1999;A260:108.
[25] Kumar KS, Pang L, Liu CT, Hoton JA, Kenik EA. Acta Mater 2000;48:911.
[26] Brady MP, Zhu JH, Liu CT, Tortorelli PF, Walker LR, McKamey CG, Wright JL, Carmichael CA, Larson DJ, Miller MK, Porter WD. Materials at High Temperatures 1999;16(4):189–93.
[27] Thoma DJ, Perepezko JH. J Alloys and Compounds 1995;224:330.
[28] Chen KC, Allen SM, Livingston JD. MRS Symp Proc 1994;364:1406.
[29] Ivey DG, Northwood DO. Z Phys Chem NF 1986;147:191.
[30] Sicking G, Magomedbekov E, Hempelmann R. Ber Bunsenges Phys Chem 1981;85:686.
[31] Zhu JH, Pike LM, Liu CT, Liaw PK. Acta Mater 1999;47:2003.
[32] Zhu JH, Liu CT. Defect structures in $ZrCo_2$ Laves phase, Acta Mater. 2000 (in press).
[33] Modder IW, Bakker H. Phys Stat Sol (b) 1997;199:369.
[34] Modder IW, Kuin MJ, Bakker H. Intermetallics 1998;6:537.
[35] Pike LM, Chang YA, Liu CT. Acta Mater 1997;45:3709.
[36] Hazzledine PM, Pirouz P. Scripta Metall Mater 1993;28:1277.
[37] Neumann JP. Acta Metall 1980;28:1165.
[38] de Boer FR, Boom R, Mattens WCM, Miedema AR, Niessen AK. Cohesion in metals and transition metal alloys, ed. de Boer FR, Pettifor DG. Vol. 1, Second Corrected Printing, North Holland, Amsterdam, 1989.
[39] Zhu JH, Liaw PK, Liu CT. Mater Sci Engng 1997;A239(240):260.
[40] Zhu JH, Liu CT, Liaw PK. Intermetallics 1999;7:1011.
[41] Bardos DI, Gupta KP, Beck PA. Trans Met Soc AIME 1961;221:1087.
[42] Massalski TB, ed. Binary alloy phase diagrams, vol. 1, ASM Publication, 1986.
[43] Thoma DJ. Unpublished results, Lawrence Livermore National Laboratory, 1998.
[44] Liu CT. Unpublished results, Oak Ridge National Laboratory, 1999.
[45] Suklyun Hong, Fu CL. in MRS Proc. vol. 552, MRS Publication, 1999:643–647.
[46] Lee S, Liaw PK, Liu CT, Chou YT. Mater Sci Engng A 1999;268:184–92.
[47] Lee S, Liaw PK, Liu CT, Chou YT. Mater Chem Phys 1999;61:207–13.
[48] Jenkins MG, Kobayashi AS, White KW, Bradt RC. Inst J Fract 1987;34:281.
[49] Schneibel JH, Carmichael CA, Specht ED, Subramanian R. Intermetallics 1997;5:61–7.
[50] Brady MP, Zhu JH, Liu CT, Tortorelli PF, Wright JL, Carmichael CA, Walker LR. Ultrahigh temperature intermetallic alloys. Proceedings of the Eleventh Annual Conference on Fossil Energy Materials, Knoxville, TN, 20–22 May, R.R. Judkins, Compiler, 1997. pp. 195–205.
[51] Brady MP, Tortorelli PF, Walker LR. Materials at high temperatures (in press).